Iizuka, Daisuke; Gon, Masayuki; Tanaka, Kazuo; Chujo, Yoshiki

Acceleration of Chemiluminescence Reactions with Coumarin-modified Polyhedral Oligomeric Silsesquioxane

Daisuke Iizuka, Masayuki Gon, Kazuo Tanaka* and Yoshiki Chujo

Department of Polymer Chemistry, Graduate School of Engineering, Kyoto University Katsura, Nishikyo-ku, Kyoto 615-8510, Japan

E-mail: <tanaka@poly.synchem.kyoto-u.ac.jp>

Kazuo Tanaka

Kazuo Tanaka received his Ph.D. degree in 2004 from Kyoto University, and worked in Stanford University, USA, Kyoto University, and RIKEN as a postdoctoral fellow. In 2007, he has moved to the Department of Polymer Chemistry, Graduate School of Engineering, Kyoto University, and in 2018, he was promoted to Professor. His research projects especially focus on design of new functional materials relating optics and nanotechnology based on the heteroatom-containing conjugated polymers and organic-inorganic polymer hybrids.

Yoshiki Chujo

Yoshiki Chujo completed his Ph.D. at Kyoto University in 1980 and then joined Nagoya University as an assistant professor in 1981. In 1983, he joined the group of J. McGrath at Virginia Polytechnic Institute as a postdoctoral research fellow. He returned to Kyoto University as a lecturer in 1986 and has been Professor of Polymer Chemistry there since 1994. In 2018, he retired from Kyoto University and was granted the title of professor emeritus. His research interests focus on polymer synthesis, inorganic polymers, and polymeric hybrid materials.

Abstract

Chemiluminescence has attracted much attention as a light source and an excitation mediator without electric power sources. To develop advanced optical materials, it is necessary to control the chemiluminescence behavior more precisely by molecular design. Herein, we describe influence of the connection to the inorganic scaffold on the chemiluminescence properties with coumarin-modified polyhedral oligomeric silsesquioxane (**D1421-POSS**). Accordingly, when **D1421-POSS** was chemically excited using bis(2-carbopentyloxy-3,5,6-trichlorophenyl) oxalate (CPPO), it was shown that the initiation of chemical emission reactions was accelerated by the POSS connection, comparing to the model compound **D1421-arm**. From cyclic voltammetry measurements, it was revealed that the oxidation potential of **D1421-POSS** was significantly lower than that of **D1421-arm**. From these data, we propose the mechanism that aggregation assisted by the POSS core induces low oxidation potential, resulting in the acceleration of chemiluminescence reactions.

Keywords: POSS, chemiluminescence, organic-inorganic hybrid

1. Introduction

Polyhedral oligomeric silsesquioxane (POSS) is a rigid molecule with a Si–O bond backbone, and its vertices can be easily modified with a variety of organic side chains.[1–3] Among them, cube-like T8 POSS (hereafter denoted as POSS for simplicity) molecules have attracted a great deal of attention for its easy synthesis as a scaffold for catalyst,[4,5] nanocomposites,[6,7] and biomaterials[8] because of unique molecular environment around the core, such as hydrophobicity and suppression of molecular motions. Most of the POSS-incorporated molecules have been used in the solid state for their excellent thermal and photo-stability.[9] Moreover, POSS-incorporated fluorescent dyes exhibited various stimuli-responsive properties in the solution state because of the interaction between guest molecules and the vacant or hydrophobic spaces created by POSS cores.[10–14] Our group has

also succeeded in identifying the *cis-trans* isomers of fatty acids,[15] the chemical compositions and sizes of nanoparticles in water,[16] and sodium dodecyl sulfate (SDS) which is the conventional indicator of river pollution[17] by utilizing the hydrophobic space of POSS. We called a series of POSS materials as designable hybrid materials based on the concept of "element-blocks", which are structural functional units composed of various groups of elements, to produce advanced materials.[18–20] As next generation of functional luminescent materials, material design from new viewpoint should be needed. In the conventional luminescent materials, photoexcitation has been used as the excitation method in almost all cases, which has the inconvenience of requiring an excitation light. In contrast, chemiluminescence is the emission of light resulted from a chemical reaction without photoexcitation.[21] It has the advantage of emitting light for a long time without any electronic power sources. Chemical excitation can be used in varieties of solutions, from organic solvents to water, and has been already widely applied as an excitation method.[22–24] Among them, bis(2-carbopentyloxy-3,5,6-trichlorophenyl) oxalate (CPPO) is a molecule that can perform efficient chemiluminescence in various solvents and is used in commercial chemical lights.[25–27] Under optimized conditions, the quantum yield can reach as high as 50%, and a variety of luminescent colors can be produced depending on the type of activators (ACT) added.[28] The mechanism of the chemical excitation of CPPO is illustrated in Figure 1. When this molecule reacts with hydrogen peroxide, it produces relatively stable high-energy intermediates (HEIs), which recently turned out to be a cyclic peroxidic carbon dioxide dimer, namely, 1,2-dioxetanedione.[29] HEI then reacts collisionally with ACT through CIEEL (chemically initiated electron exchange luminescence) mechanism to produce an excited state (Scheme 1).[28,30,31] In this CIEEL mechanism, the cleavage of O–O bond occurs almost simultaneously with the electron transfer from HEI to ACT. Then, when the C–C bond is ruptured, CO_2 leaves and a pair of a radical anion of CO_2 and the radical cation of ACT is generated. Finally, the excess energy is released by back energy transfer, and subsequently the ACT is excited to the singlet

excited state. It is known that the oxidation of ACT is the rate-limiting step of this reaction, which means the oxidation potential of ACT dye significantly affects the reaction rate.

In this study, we investigated the chemiluminescence properties of coumarin-modified POSS (**D1421-POSS**), which was easily synthesized by the condensation reaction of coumarin D1421 and an octaammonium-substituted POSS. The dye molecule corresponding to one side chain of POSS (**D1421-arm**) were used as a model compound to evaluate the effect of POSS by comparing the various physical properties. When these molecules were chemiexcited using CPPO, it was revealed that the chemiluminescence of **D1421-POSS** was faster than that of the **D1421-arm**. Cyclic voltammetry revealed that the oxidation potential of **D1421-POSS** was lower than that of **D1421-arm**, which led to the increase in the reaction rate of chemiluminescence. It is implied that aggregation assisted by POSS might play a key role in this acceleration effect. Although there has been a report on chemical excitation of POSS,[32] to the best of our knowledge, this is the first paper to demonstrate the regulation of chemiluminescence kinetics by employing the molecular scaffold as well as POSS.
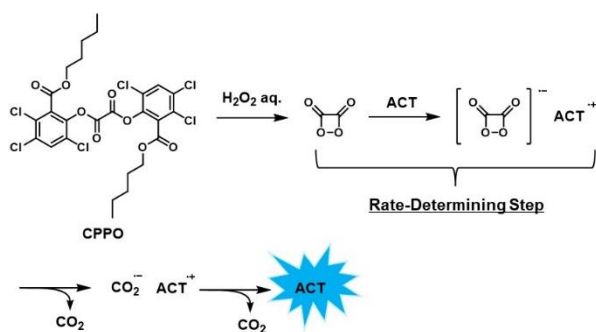

Figure 1. Chemiexcitation mechanism of CPPO.

2. Experimental

Materials. Propylamine, 4-(diethylamino)salicylaldehyde was purchased from Tokyo Chemical Industry Co, Ltd. *N*,*N*-Diisopropylethylamine (DIEA), meldrum's acid, 4-(4,6-dimethoxy-1,3,5-triazin-2-yl)-4-methylmorpholinium chloride (DMT-MM) and hydrogen peroxide (30.0-35.5%, mass/mass) were purchased from FUJIFILM Wako Pure Chemical Corporation. 1-[Bis(dimethylamino)methylene]-1*H*-benzotriazolium 3-oxide hexafluorophosphate (HBTU) was purchased from PEPTIDE INSTITUTE, INC. *N*,*N*-Dimethylformamide (DMF), dimethyl sulfoxide (DMSO), and all commercial materials were used without purification. Triethylamine (Et₃N) (Kanto Chemical Co., Inc.) was purified by passage through solvent purification columns under N₂ pressure. Octakis(3-aminopropyl) POSS
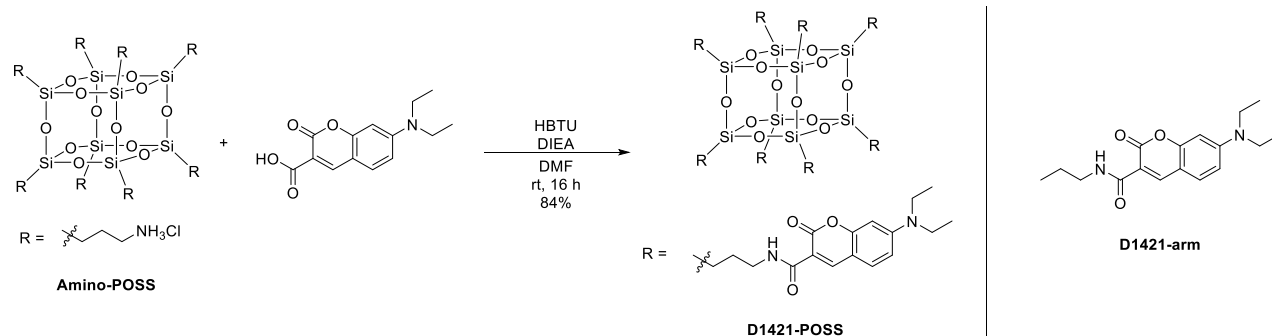
hydrochloride (**Amino-POSS**),[33] 7-(diethylamino)coumarin-3-carboxylic acid (D1421),[34] and **D1421-arm**[16] were synthesized according to the literatures.

Methods. ^{1}H, ^{13}C and ^{29}Si NMR spectra were recorded on JEOL EX400 and AL400 instruments at 400, 100 and 80 MHz respectively. Samples were analyzed in CDCl₃. The chemical shift values were expressed relative to Me₄Si as an internal standard in CDCl₃. High-resolution mass (HRMS) spectrometry was performed on an EXACTIVE Plus (Thermo Fisher Scientific) at the Technical Support Office (Department of Synthetic Chemistry and Biological Chemistry, Graduate School of Engineering, Kyoto University), and the high-resolution mass spectra (HRMS) were obtained on a Thermo Fisher EXACTIVE for electrospray ionization (ESI). UV–vis spectra were recorded on a SHIMADZU UV-3600i Plus spectrophotometer, and samples were analyzed at room temperature. Fluorescence emission spectra were measured with a HORIBA JOBIN YVON Fluorolog-3 spectrofluorometer. Absolute photoluminescence quantum efficiency (Φ_{PL}) was recorded on a Hamamatsu Photonics Quantaurus-QY Plus C13534-01. Elemental analyses were performed with a MICRO CORDER MT-5 (YANACO CO.,Ltd.) at the Microanalytical Center of Kyoto University. Thermogravimetric analysis (TGA) was recorded on a Hitachi High-Tech Science Corporation. TA STA7200RV. Cyclic voltammetry (CV) was carried out on a BAS ALS-Electrochemical-Analyzer Model 600D with a glassy carbon working electrode, a Pt counter electrode, an Ag/Ag⁺ reference electrode, and the ferrocene/ferrocenium external reference at a scan rate of 0.1 V s⁻¹. The dynamic light scattering (DLS) measurements were carried out at 90° scattering angle and 20 ± 0.2 °C using a FPAR-1000 particle analyzer with a He-Ne laser as a light source. The CONTIN program was used for data analysis to extract information on the average hydrodynamic size. All reactions were performed under nitrogen atmosphere.

3. Results and Discussion

Synthetic Procedure. Scheme 1 shows the synthetic route for **D1421-POSS**. We chose D1421 as a fluorophore because of its high photoluminescence quantum yield and designability via carboxylic acid. **D1421-POSS** was synthesized by a condensation reaction of octakis(3-aminopropyl) POSS hydrochloride (**Amino-POSS**) and D1421 in 84% isolated yield. The completely eight-substituted POSS was precipitated under the reaction and collected simply by filtration. Figure S1 shows the ^{1}H NMR spectrum of **D1421-POSS**. From the integration ratio of the signal peak from the singlet amide proton (8.62 ppm), it was revealed that eight D1421 units can be covalently attached to the POSS moiety. The signal at –66.9 ppm in the ^{29}Si NMR spectrum indicates that the cubic POSS cage should remain intact (Figure S3). The FT-IR spectra of

Scheme 1. Synthetic route to **D1421-POSS** and chemical structure of **D1421-arm**.

D1421-POSS and **D1421-arm** are shown in Figure S4. Differently from **D1421-arm**, **D1421-POSS** exhibited a peak at 1097 cm^{-1} corresponding to Si–O stretching vibration. The structure was also confirmed by ^{13}C NMR spectroscopy (Figure S2), a high-resolution mass spectrometry and an elemental analysis.
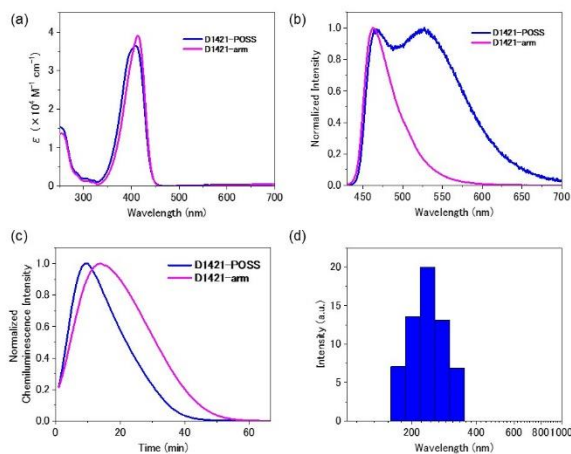
Figure 2. (a) Absorption (8.0×10^{-6} M for D1421 unit) and (b) emission spectra of **D1421-POSS** and **D1421-arm**. (c) The curves of chemiluminescence intensity vs. time. (d) Number-averaged hydrodynamic size distribution of **D1421-POSS**. All measurements were conducted in THF/CHCl$_3$/H$_2$O(H$_2$O$_2$ aq. for Figure 2c) = 2.7/0.3/0.1 mixed solution (8.0×10^{-4} M for D1421 unit).

Table 1. Oxidation potentials of **D1421-POSS** and **D1421-arm**

	Oxidation Potential (V)
D1421-POSS	0.50
D1421-arm	0.61

^{a} Measured in THF/CHCl$_3$/H$_2$O = 2.7/0.3/0.1 solution (8.0×10^{-4} M for D1421 unit).

Photophysical Characterization. The photoluminescence properties of **D1421-POSS** and **D1421-arm** were measured in the THF/CHCl$_3$/H$_2$O = 2.7/0.3/0.1 mixed solutions. THF was a poor solvent for **D1421-POSS**. To form a stable aggregation of **D1421-POSS**, a small amount of CHCl$_3$ (good solvent for D1421-POSS) was required. In addition, THF was able to mix H$_2$O which was needed to introduce H$_2$O$_2$ for chemiluminescence. From the dynamic light scattering (DLS) measurements, we found that **D1421-POSS** has a number-weighted hydrodynamic size of 240.8 ± 40.6 nm (Figure 2d) with macroscopic homogeneousness good for manipulation in this chemiluminescence solvent system, while apparent aggregate was hardly detected with **D1421-arm** for its good solubility. Figures 2a and 2b and Table 1 present the UV–vis absorption and emission spectra of **D1421-POSS** and **D1421-arm**. The wavelengths of absorption maximum (λ_{abs}) of **D1421-POSS** and **D1421-arm** were 409 and 414 nm, respectively. Compared to **D1421-arm**, the blue-shifted and broader absorption band with slight decrease in a molar extinction coefficient (ε) were observed in **D1421-POSS** than that of **D1421-arm**, implying that inter- or intramolecular interaction between D1421 moieties could be enhanced in the presence of POSS because similar spectra was observed even in the diluted chloroform solution as good solvent (Figure S6a). Although both **D1421-POSS** and **D1421-arm** had the emission

band with the peak (λ_{em}) around 465 nm, only **D1421-POSS** had another much longer emission band with the peak at 526 nm. Recently, emission originating from the transition from the TICT state of the coumarin derivatives was reported to become emissive under specific environments where the molecular motion was suppressed by hydrogen bonds such as around the upper rim of γ-CD[35] and water-soluble POSS networks.[16] In our case, it is suggested that the nano-sized aggregation and accumulation of eight coumarins should be responsible for suppression of molecular vibration, resulting in the emission obtained from the transition from the TICT state. Such yellow luminescence was also observed in the diluted chloroform solution, indicating the existence of intramolecular restriction between side chains although the intensity ratio was smaller than that in the submicron aggregated condition (THF/CHCl$_3$/H$_2$O mixed solution).

Thermal Properties. The connection with POSS can be expected to enhance thermal stability of coumarin dyes by suppressing molecular motions. The decomposition temperatures (T_d) of **D1421-POSS** and **D1421-arm** were determined by thermogravimetric analysis (TGA) in N$_2$ atmosphere (Figure S8). The T_d of **D1421-POSS** was found to be 384.6 °C, which is more than 100 °C higher than that of the model compound. A differential scanning calorimetry (DSC) study was also conducted (Figure S9). The melting points of **D1421-POSS** and **D1421-arm** were determined as 283.4 °C and 132.8 °C, respectively. After the 1st heat step of **D1421-POSS**, no crystallization and melting peaks were observed during cooling and heating cycles. It is likely that amorphous state should be maintained due to its dendritic structure once **D1421-POSS** is melted. Instead of the crystallization and melting, **D1421-POSS** showed glass transition at around 73 °C. These results clearly indicate that POSS plays a critical role in improving thermal stability and suppressing phase transition to crystalline state. Reinforcement of thermal stability is favorable for stable use of chemiluminescence.

Chemiluminescence Study The chemiluminescence behavior was investigated using CPPO. The chemiluminescence samples consisted of 1.0×10^{-4} M **D1421-POSS** (or 8.0×10^{-4} M **D1421-arm**) and 1.0×10^{-2} M CPPO, which produced chemiluminescence upon adding the H$_2$O$_2$ aqueous solution (30.0-35.5％). The chemiluminescence spectra were identical to the photoluminescence spectra (Figure S5). We monitored the time-courses of intensity changes to evaluate the effect of the POSS moiety (Figure 2c). Interestingly, the onset of the chemiluminescence of **D1421-POSS** was faster than that of the **D1421-arm**. In 2000, Baader and co-workers reported that the chemiluminescence in peroxyoxalate systems was faster when the oxidation potential of ACT was lower,[28] which motivated us to carry out cyclic voltammetry (CV). The oxidation potentials of **D1421-POSS** and **D1421-arm** were found to be 0.50 and 0.61 V respectively (Table 1). From these data, we concluded that this lower oxidation potential of **D1421-POSS** accelerated the chemiluminescence reaction. In general, the accumulation of dyes into POSS is expected to reduce the diffusion coefficient and slow down the electrochemical response. However, in **D1421-POSS**, the opposite result was obtained. To gain insight on this lowering effect of POSS on oxidation potential, we performed additional experiments.

We speculated that the lower oxidation potential of **D1421-POSS** might be induced due to aggregate formation. To examine the influence of aggregation on electrochemical properties, DLS and CV measurements were implemented

using chloroform or dichloromethane as good solvents (Figure S11). The results showed that neither aggregation nor the difference in oxidation potential between POSS and the model compound was detected. These results suggest that the aggregation formation of POSS may have caused some intermolecular interactions in the D1421 unit, leading to decrease in the oxidation potential.

4. Conclusion

In conclusion, we have investigated chemiluminescence from coumarin-modified POSS. We prepared POSS modified with eight coumarin D1421 units by a simple synthetic procedure. By connecting with POSS and making submicron aggregates, D1421 emitted faster when chemiexcited with CPPO. This interesting result was successfully explained by the difference in the oxidation potential experimentally estimated from CV. Our findings propose that dye accumulation with the POSS core could be the potential strategy for regulating kinetics of chemiluminescence through the aggregation-supported acceleration effect.

References

1 D. B. Cordes, P. D. Lickiss, F. Rataboul, *Chem. Rev.* **2010**, *110*, 2081.

2 Z. Li, J. Kong, F. Wang, C. He, *J. Mater. Chem. C* **2017**, *5*, 5283.

3 K. Tanaka, Y. Chujo, *J. Mater. Chem.* **2012**, *22*, 1733.

4 M. G. Schwab, M. Hamburger, X. Feng, J. Shu, H. W. Spiess, X. Wang, M. Antonietti, K. Müllen, *Chem. Commun.* **2010**, *46*, 8932.

5 W.-J. Wang, K.-H. Chen, Z.-W. Yang, B.-W. Peng, L.-N. He, *J. Mater. Chem. A* **2021**, *9*, 16699.

6 S.-W. Kuo, F.-C. Chang, *Prog. Polym. Sci.* **2011**, *36*, 1649.

7 A. Fina, O. Monticelli, G. Camino, *J. Mater. Chem.* **2010**, *20*, 9297.

8 R. Y. Kannan, H. J. Salacinski, P. E. Butler, A. M. Seifalian, *Acc. Chem. Res.* **2005**, *38*, 879.

9 K. L. Chan, P. Sonar, A. Sellinger, *J. Mater. Chem.* **2009**, *19*, 9103.

10 K. Xiang, Y. Li, C. Xu, S. Li, *J. Mater. Chem. C* **2016**, *4*, 5578.

11 H. Zhou, Q. Ye, X. Wu, J. Song, C. M. Cho, Y. Zong, B. Z. Tang, T. S. A. Hor, E. K. L. Yeow, J. Xu, *J. Mater. Chem. C* **2015**, *3*, 11874.

12 K. Xiang, L. He, Y. Li, C. Xu, S. Li, *RSC Adv.* **2015**, *5*, 97224.

13 H. Liu, H. Liu, *J. Mater. Chem. A* **2017**, *5*, 9156.

14 R. Majumdar, C. Wannasiri, M. Sukwattanasinitt, V. Ervithayasuporn, *Polym. Chem.* **2021**, *12*, 3391.

15 H. Narikiyo, T. Kakuta, H. Matsuyama, M. Gon, K. Tanaka, Y. Chujo, *Bioorg. Med. Chem.* **2017**, *25*, 3431.

16 R. Nakamura, H. Narikiyo, M. Gon, K. Tanaka, Y. Chujo, *Mater. Chem. Front.* **2019**, *3*, 2690.

17 H. Narikiyo, M. Gon, K. Tanaka, Y. Chujo, *Mater. Chem. Front.* **2018**, *2*, 1449.

18 M. Gon, K. Tanaka, Y. Chujo, *Polym. J.* **2018**, *50*, 109.

19 Y. Chujo, K. Tanaka, *Bull. Chem. Soc. Jpn.* **2015**, *88*, 633.

20 K. Tanaka, Y. Chujo, *Polym. J.* **2020**, *52*, 555.

21 L. J. Kricka, *Clin. Chem.* **1991**, *37*, 1472.

22 H. Chen, L. Lin, H. Li, J.-M. Lin, *Coord. Chem. Rev.* **2014**, *263–264*, 86.

23 Y. Su, D. Deng, L. Zhang, H. Song, Y. Lv, *TrAC Trends Anal. Chem.* **2016**, *82*, 394.

24 M. Iranifam, *TrAC Trends Anal. Chem.* **2014**, *59*, 156.

25 Y. Yang, S. Wang, L. Lu, Q. Zhang, P. Yu, Y. Fan, F. Zhang, *Angew. Chem. Int. Ed.* **2020**, *59*, 18380.

26 Y. Wang, L. Shi, Z. Ye, K. Guan, L. Teng, J. Wu, X. Yin, G. Song, X.-B. Zhang, *Nano Lett.* **2020**, *20*, 176.

27 Y.-D. Lee, C.-K. Lim, A. Singh, J. Koh, J. Kim, I. C. Kwon, S. Kim, *ACS Nano* **2012**, *6*, 6759.

28 C. V. Stevani, S. M. Silva, W. J. Baader, *European J. Org. Chem.* **2000**, 4037.

29 S. M. da Silva, A. P. Lang, A. P. F. dos Santos, M. C. Cabello, L. F. M. L. Ciscato, F. H. Bartoloni, E. L. Bastos, W. J. Baader, *J. Org. Chem.* **2021**, *86*, 11434.

30 G. B. Schuster, *Acc. Chem. Res.* **1979**, *12*, 366.

31 J.-Y. Koo, G. B. Schuster, *J. Am. Chem. Soc.* **1977**, *99*, 6107.

32 M. Sun, Y. Su, W. Yang, L. Zhang, J. Hu, Y. Lv, *Anal. Chem.* **2019**, *91*, 8926.

33 K. Tanaka, K. Inafuku, S. Adachi, Y. Chujo, *Macromolecules* **2009**, *42*, 3489.

34 H. G. Ghalehshahi, S. Balalaie, A. Aliahmadi, *New J. Chem.* **2018**, *42*, 8831.

35 B. Maity, A. Chatterjee, S. A. Ahmed, D. Seth, *J. Lumin.* **2017**, *183*, 238.

Graphical Abstract

<Title>

Acceleration of Chemiluminescence Reactions with Coumarin-modified Polyhedral Oligomeric Silsesquioxane

<Authors' names>

Daisuke Iizuka, Masayuki Gon, Kazuo Tanaka* and Yoshiki Chujo

<Summary>

To develop advanced optical materials, it is necessary to control the chemiluminescence behavior more precisely by molecular design. Herein, we describe the influence of the connection to the inorganic scaffold on the chemiluminescence properties with coumarin-modified polyhedral oligomeric silsesquioxane (POSS). Accordingly, we found that the initiation of chemiluminescence reactions was accelerated using POSS.

<Diagram>

Chemiluminescence
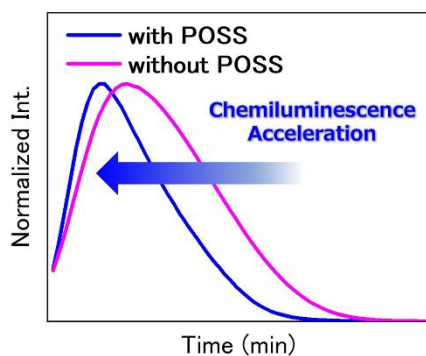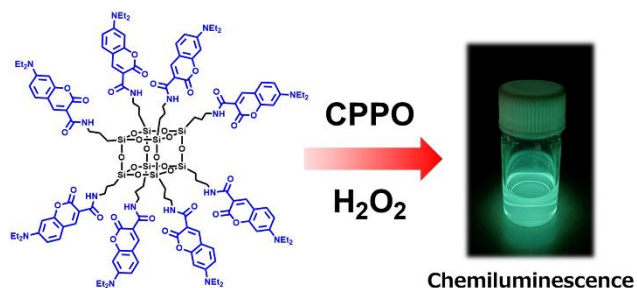
Supporting Information

Acceleration of Chemiluminescence Reactions with Coumarin-modified Polyhedral Oligomeric Silsesquioxane

Daisuke Iizuka, Masayuki Gon, Kazuo Tanaka* and Yoshiki Chujo

Department of Polymer Chemistry, Graduate School of Engineering, Kyoto University Katsura, Nishikyo-ku, Kyoto 615-8510, Japan

E-mail: tanaka@poly.synchem.kyoto-u.ac.jp

Contents page

Synthetic Procedures and Characterization

Scheme 1. Synthesis of D1421-POSS
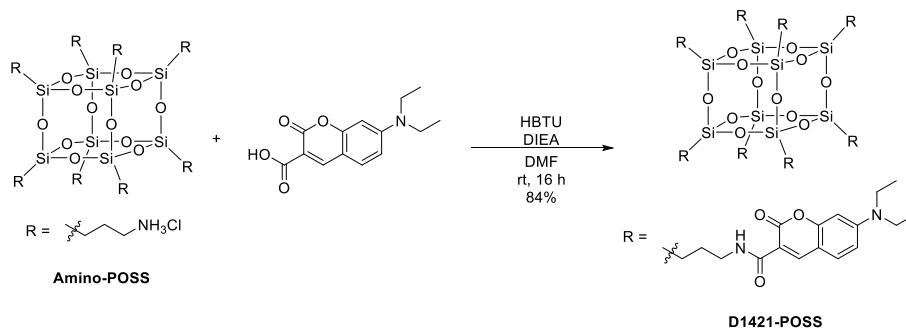
Coumarin D1421 (523.0 mg, 2.00 mmol) and HBTU (910.0 mg, 2.4 mmol) were placed in a round-bottom flask equipped with a magnetic stirring bar. DMF (20 mL) and DIEA (0.836 mL, 4.8 mmol) were added to the flask and the mixture was cooled on an ice bath. After the mixture was activated at room temperature for 30 min, **Amino-POSS** (235.0 mg, 0.200 mmol) was added to this solution and stirred for 16 h. The precipitate was collected by filtration, washed with DMF and dried *in vacuo*. The yellow solid of **D1421-POSS** (474 mg, 0.168 mmol, 84%) was then obtained.

^{1}H NMR (400 MHz, CDCl$_3$) δ 8.75 (t, J = 2.1 Hz, 1H), 8.62 (s, 1H), 7.34 (d, J = 8.8 Hz, 1H), 6.54 (dd, J = 8.9, 2.3 Hz, 1H), 6.40 (d, J = 2.2 Hz, 1H), 3.44-3.35 (m, 6H), 1.74 (q, J = 7.6 Hz, 2H), 1.18 (t, J = 7.1 Hz, 6H), 0.73 (t, J = 8.3 Hz, 2H) ppm; ^{13}C NMR (CDCl$_3$, 100 MHz) δ 162.8, 162.4, 157.5, 152.11, 147.7, 131.0, 111.2, 109.5, 108.5, 96.6, 45.0, 42.2, 23.0, 12.4, 9.4 ppm; ^{29}Si NMR (CDCl$_3$, 80 MHz) δ −66.9 (s) ppm. HRMS (ESI) calcd. for C$_{136}$H$_{168}$N$_{16}$O$_{36}$Si$_8$ + Na [M+Na]$^+$: 2847.9853, found: 2847.9888. Elemental analysis calcd. for C$_{136}$H$_{168}$N$_{16}$O$_{36}$Si$_8$: C 57.77 H 5.99 N 7.93, found: C 57.59 H 5.92 N 7.91.
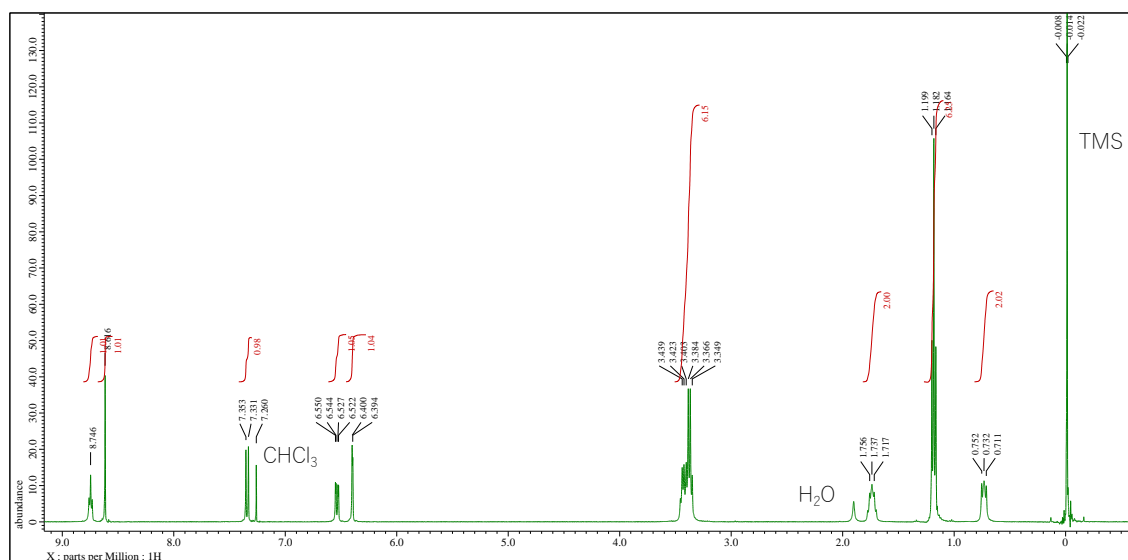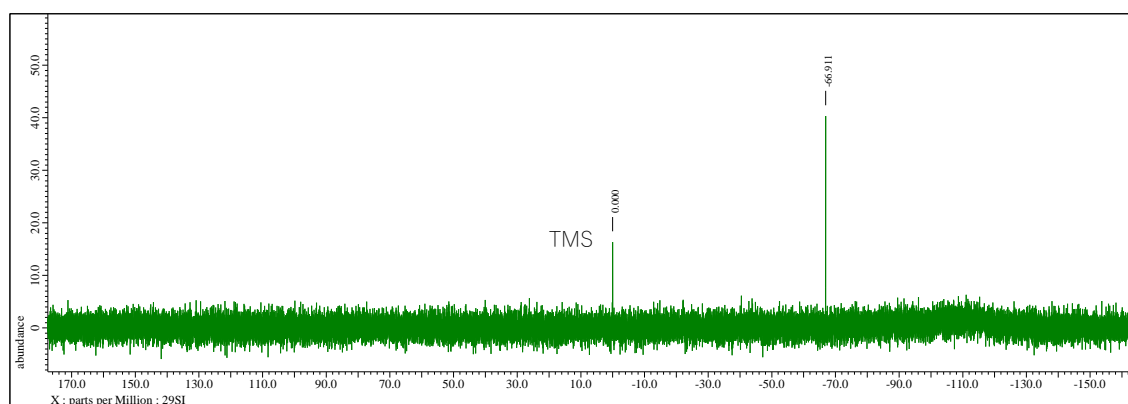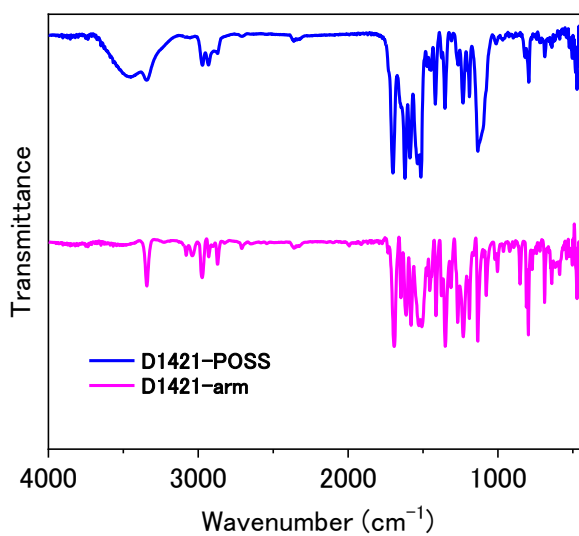
Figure S1. ^{1}H NMR spectrum of **D1421-POSS** in CDCl$_3$.
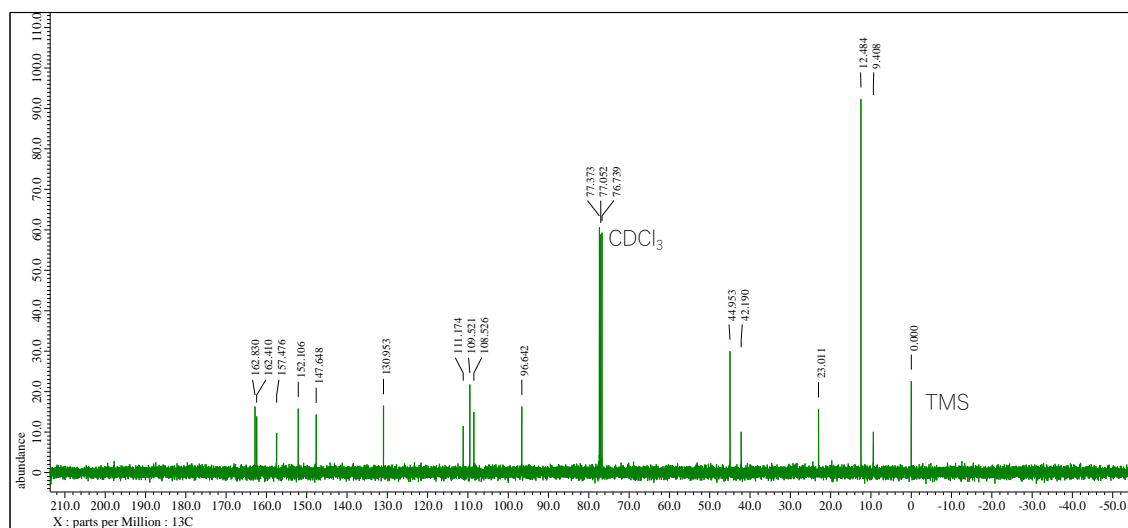
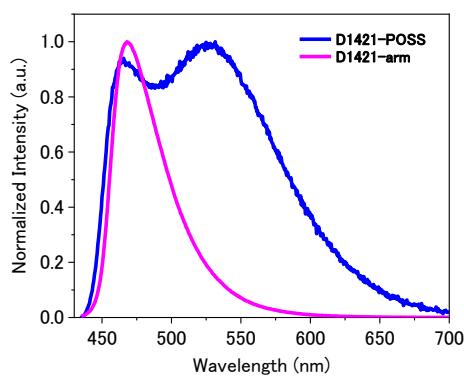

Figure S2. ^{13}C NMR spectrum of **D1421-POSS** in CDCl$_3$.

Figure S3. ^{29}Si NMR spectrum of **D1421-POSS** in CDCl$_3$.
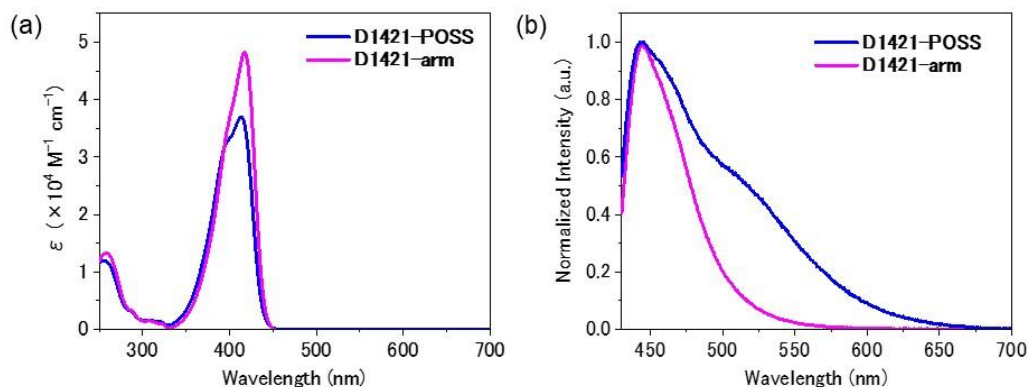
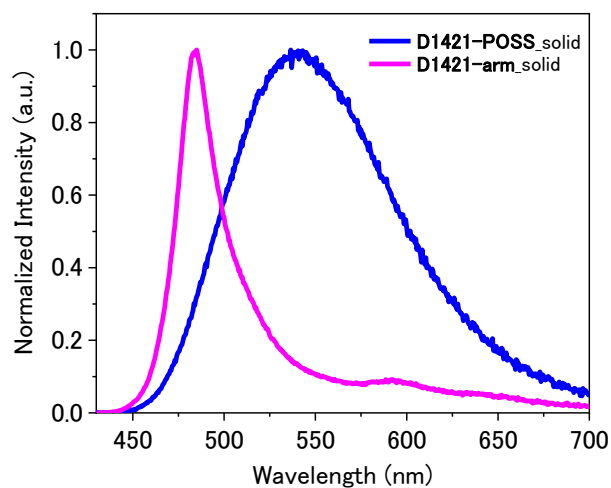**Figure S4.** IR spectra of **D1421-POSS** and **D1421-arm** in KBr pellets.

Optical data of compounds in solution and solid states

Figure S5. Chemiluminescence spectra of **D1421-POSS** and **D1421-arm** in THF/CHCl$_3$/H$_2$O$_2$ aq. = 2.7/0.3/0.1 (8.0×10^{-4} M for a D1421 unit).

Figure S6. (a) Absorption and (b) emission spectra of **D1421-POSS** and **D1421-arm** in solution (CHCl$_3$, 8.0×10^{-6} M for D1421 unit).

Figure S7. Emission spectra of **D1421-POSS** and **D1421-arm** in solid state**.**

Electronic Supporting Information for *Bulletin of the Chemical Society of Japan*
© 2021 The Chemical Society of Japan

Table S1. Optical data of **D1421-POSS** and **D1421-arm** in solution and solid states

		λ_{max}^{abs} (nm)	λ_{max}^{em} (nm)^c	ε (M^{-1} cm^{-1})^d	Φ_{PL} (%)
D1421-POSS	THF/CHCl$_3$/H$_2$O^a	409	467, 527	36,500	14
	CHCl$_3$^{b}	413	446	37,000	39
	solid	-	541	-	16
D1421-arm	THF/CHCl$_3$/H$_2$O^a	414	462	39,100	29
	CHCl$_3$^{b}	417	444	48,200	97
	solid	-	485	-	27

^{a} In THF/CHCl$_3$/H$_2$O = 27/3/1 solution, 1.0×10^{-6} M for D1421 unit (absorption), 1.0×10^{-4} M for D1421 unit (emission and Φ_{PL}).

^{b} 1.0×10^{-6} M for D1421 unit (absorption), 1.0×10^{-4} M for D1421 unit (emission and Φ_{PL}).
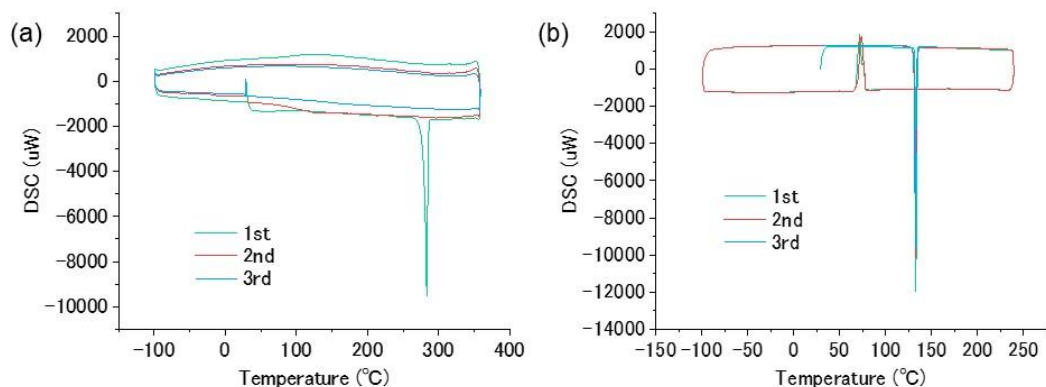
^{c} Excited at the wavelengths of absorption maxima (λ_{abs}).

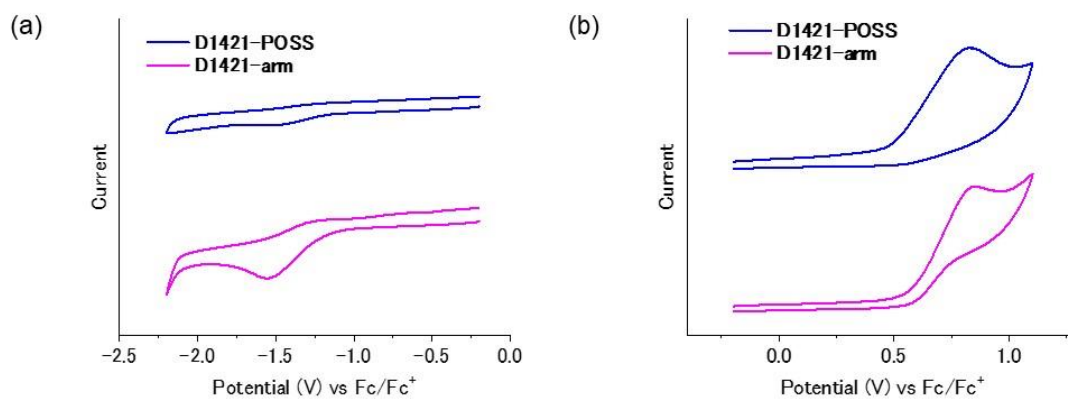^{d} Calculated based on the concentration of D1421 unit.

Thermal analysis
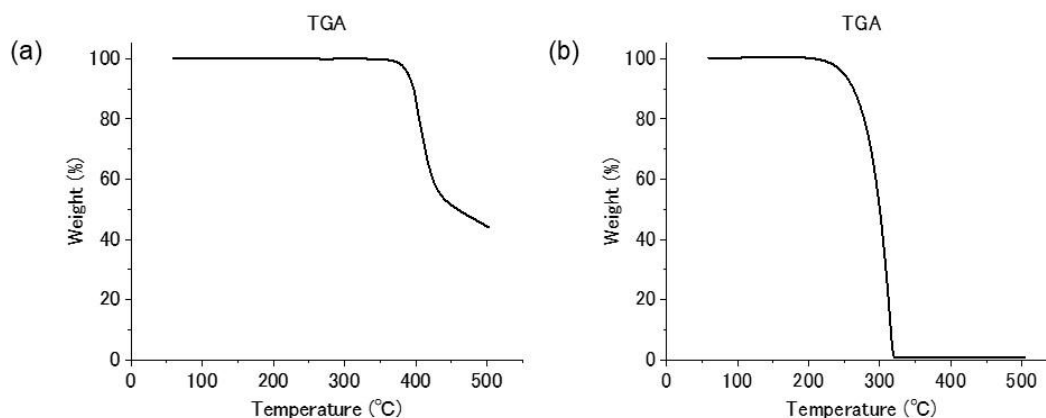
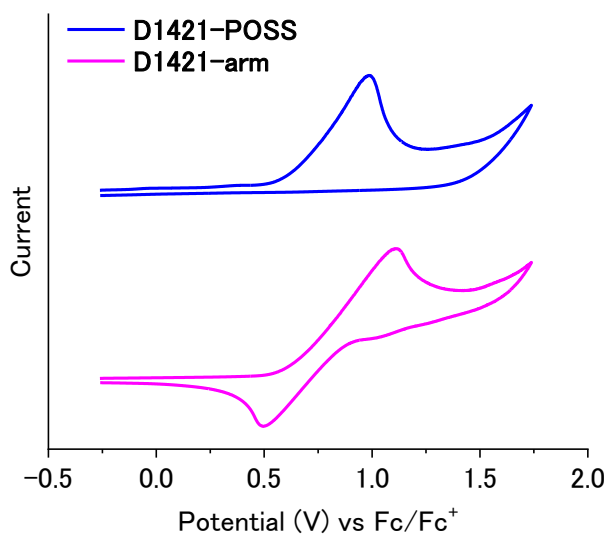**Figure S8.** TGA curves of (a) **D1421-POSS** and (b) **D1421-arm**.

Figure S9. DSC thermograms of (a) **D1421-POSS** and (b) **D1421-arm**.

Cyclic voltammetry measurement

Figure S10. Voltammograms of **D1421-POSS** and **D1421-arm** in (a) negative (b) positive scans. (8.0 × 10^{-4} M for D1421 unit in THF/CHCl$_3$/H$_2$O = 2.7/0.3/0.1)

京都大学
KYOTO UNIVERSITY

京都大学学術情報リポジトリ
KURENAI 紅
Kyoto University Research Information Repository

Electronic Supporting Information for *Bulletin of the Chemical Society of Japan*
© 2021 The Chemical Society of Japan

Figure S11. Voltammograms of **D1421-POSS** and **D1421-arm** in positive scans (8.0×10^{-4} M for D1421 in dichloromethane).

<Start Description of your Supporting Information from this page>